0026-895X/11/8003-378–388$25.00
MOLECULAR PHARMACOLOGY
Copyright © 2011 The American Society for Pharmacology and Experimental Therapeutics
Mol Pharmacol 80:378–388, 2011

Vol. 80, No. 3
72991/3705505
Printed in U.S.A.

Allosteric Modulation of the M_3 Muscarinic Receptor by Amiodarone and *N*-Ethylamiodarone: Application of the Four-Ligand Allosteric Two-State Model

Edward Stahl, Gwendolynne Elmslie, and John Ellis

Departments of Psychiatry and Pharmacology, the Penn State University College of Medicine, Hershey, Pennsylvania

Received April 21, 2011; accepted May 20, 2011

ABSTRACT

We have reported previously that amiodarone interacts with muscarinic receptors via a novel allosteric site. This study presents mechanistic details on the nature of that interaction. Amiodarone enhanced the maximal level of agonist-stimulated release of arachidonic acid (AA) from Chinese hamster ovary cells that expressed M_3 muscarinic receptors; this enhancement was observed for acetylcholine and for the partial agonist pilocarpine. A similar effect of amiodarone was observed when pilocarpine was used to stimulate inositol phosphate (IP) metabolism, but not when acetylcholine was used. Subsequent studies showed that the IP response exhibited a much larger receptor reserve than the AA response, and reduction of that reserve by receptor alkylation unmasked amiodarone's enhancement of the maximal IP response to acetylcholine. Modulating the receptor reserve also revealed acetylcholine's greater affinity (K_A) for the conformation of the receptor that mediates the AA response. The amiodarone analog *N*-ethylamiodarone (NEA) did not alter maximal agonist response but merely reduced agonist potency (that is, it appeared to be an antagonist). However, the action of NEA could be clearly distinguished from the action of the orthosteric antagonist NMS. Demonstration of this point was facilitated by an elaboration of Hall's allosteric two-state model; this new model represents a system composed of two ligands that compete with each other at the orthosteric site and two ligands that compete with each other at the allosteric site. In conclusion, amiodarone competes with NEA at a novel, extracellular, allosteric site to enhance the maximal stimulation evoked by acetylcholine and pilocarpine in two different responses.

Introduction

Allosteric modulation uses receptor sites that are physically distinct from the orthosteric site; the orthosteric site is the binding site for the endogenous hormone or neurotransmitter. Targeting these alternate sites provides several potential benefits over the conventional approach of developing orthosterically acting ligands. The benefits can include increased receptor subtype selectivity, decreased toxicity, and the ability to retain spatial and temporal signal patterning (Ellis, 1997; Bridges and Lindsley, 2008). The muscarinic acetylcholine (ACh) receptor family has become a model system for allosteric interactions of class A G protein-coupled receptors (GPCRs), partly because a great deal is known about the location of one of the muscarinic allosteric sites (May et al., 2007). All of the muscarinic receptors are susceptible to allosteric modulation and, for a subset of allosteric ligands, a "common site" has been established. The ligands shown to act at this common site include gallamine, obidoxime, alcuronium, strychnine, and hexamethylene-bis-[dimethyl-(3-phthalimidopropyl)ammonium]dibromide (W84) (Ellis and Seidenberg, 2000; Tränkle et al., 2003). Moreover, the high degree of sequence homology in the orthosteric acetylcholine binding site has impeded the development of useful subtype-selective orthosteric ligands (Jones et al., 1992). It is believed that targeting regions of the receptor with greater sequence divergence (i.e., allosteric sites) will facilitate the discovery of more subtype-selective compounds and allow therapeutic exploitation of the different subtypes (Wess et al., 2007; Langmead et al., 2008). In agreement with this view, the current set of subtype-selective ligands generally

This work was supported by the National Institutes of Health National Institute on Aging [Grant R01-AG05214].
Article, publication date, and citation information can be found at http://molpharm.aspetjournals.org.
doi:10.1124/mol.111.072991.

ABBREVIATIONS: ACh, acetylcholine; GPCR, G protein-coupled receptor; W84, hexamethylene-bis-[dimethyl-(3-phthalimidopropyl)ammonium] dibromide; ATSM, allosteric two-state model; TCM, ternary complex model; CTCM, cubic ternary complex model; NMS, *N*-methylscopolamine; PAM, positive allosteric modulator; 4L-ATSM, four-ligand allosteric two-state model; NEA, *N*-ethylamiodarone; AA, arachidonic acid; PB, phosphate buffer; PBS, phosphate-buffered saline; CHO, Chinese hamster ovary; EM-BSA, Eagle's basal medium with 20 mM HEPES and 2 mg/ml fatty acid-free bovine serum albumin; IP, inositol phosphate; POB, phenoxybenzamine ; NAM, negative allosteric modulator.

act at allosteric sites (Shirey et al., 2008; Bridges et al., 2009; Marlo et al., 2009).

Several models have been proposed to describe how an allosteric ligand can affect a receptor's binding and response profile (Weiss et al., 1996; Christopoulos and Kenakin, 2002; Ehlert, 2005). The allosteric two-state model (ATSM; Fig. 1) is a mechanistic representation of allosteric modulation of response (Hall, 2000). It is an extension of the two-state model (for review, see Leff, 1995) that incorporates and builds on the ternary complex model (TCM; Stockton et al., 1983; Ehlert, 1988) used to describe multiple receptor binding states attained in the presence of both an allosteric and an orthosteric ligand. In the ATSM, additional receptor states provide the model with the flexibility to address novel forms of ligand-receptor interaction, whereas multiple cooperativity parameters provide useful means for describing allosteric modulation. The ATSM is formally equivalent to the cubic ternary complex model (CTCM) of Weiss et al. (1996), although, as Hall (2000) has pointed out, the interpretations of some of the parameters differ markedly in the two models. As such, the ATSM reflects both the disadvantages and the advantages of the CTCM; that is, its complexity makes it more suitable for descriptive simulation than for parameter estimation, but it provides a representation of allosteric modulation that is entirely consistent with mechanistic principles of receptor activation. As Weiss et al. (1996) articulated, these models possess "an elegance that can be described in four words: comprehensiveness, symmetry, generalizability, and completeness."

We have characterized the allosteric effects of amiodarone on muscarinic receptors and established that it interacts with a novel site (Stahl and Ellis, 2010). An enhancement of the M_5 response was observed for a number of full and partial muscarinic agonists, including ACh. When amiodarone was included in ACh concentration-response curves, there was an increase in the level of maximum response elicited from M_5 receptors. The allosteric nature of this interaction was supported by binding studies demonstrating that amiodarone did not interact with the orthosteric ACh binding site.

The goal of this study was to develop a more complete understanding of the allosteric effects of amiodarone by focusing on the M_3 receptor. We begin by showing that amiodarone inhibits the binding of *N*-methylscopolamine (NMS) in an allosteric manner at the M_3 subtype. Despite this negative cooperativity toward NMS, we refer to amiodarone as a positive allosteric modulator (PAM) throughout this article on the basis of its ability to enhance functional responses to the endogenous agonist ACh. Two different re-

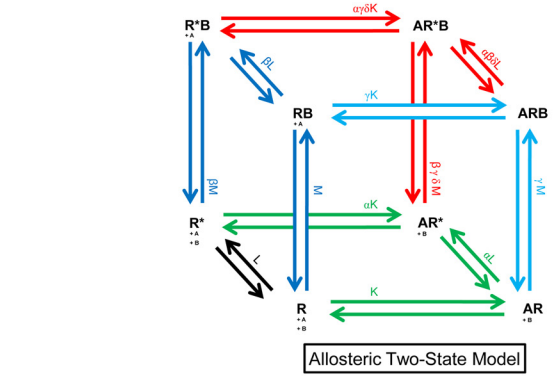

$$\text{Response}=\frac{L(1+\alpha KA+\beta MB+\alpha\beta\gamma\delta KAMB)}{1+KA+MB+\gamma KAMB+L(1+\alpha KA+\beta MB+\alpha\beta\gamma\delta KAMB)}$$

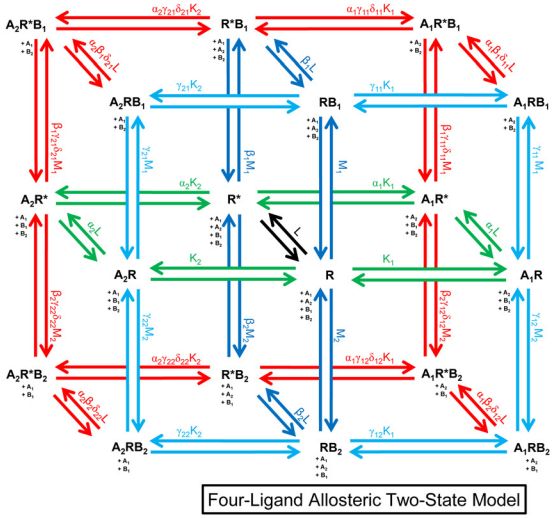

$$\text{Response}=\frac{\begin{array}{c}L(1+\alpha_1K_1A_1+\alpha_2K_2A_2+\beta_1M_1B_1+\beta_2M_2B_2\\+\alpha_1\beta_1\gamma_{11}\delta_{11}K_1A_1M_1B_1+\alpha_2\beta_1\gamma_{21}\delta_{21}K_2A_2M_1B_1\\+\alpha_1\beta_2\gamma_{12}\delta_{12}K_1A_1M_2B_2+\alpha_2\beta_2\gamma_{22}\delta_{22}K_2A_2M_2B_2)\end{array}}{\begin{array}{c}1+K_1A_1+K_2A_2+M_1B_1+M_2B_2\\+\gamma_{11}K_1A_1M_1B_1+\gamma_{12}K_1A_1M_2B_2+\gamma_{21}K_2A_2M_1B_1+\gamma_{22}K_2A_2M_2B_2\\+L(1+\alpha_1K_1A_1+\alpha_2K_2A_2+\beta_1M_1B_1+\beta_2M_2B_2\\+\alpha_1\beta_1\gamma_{11}\delta_{11}K_1A_1M_1B_1+\alpha_1\beta_2\gamma_{12}\delta_{12}K_1A_1M_2B_2\\+\alpha_2\beta_1\gamma_{21}\delta_{21}K_2A_2M_1B_1+\alpha_2\beta_2\gamma_{22}\delta_{22}K_2A_2M_2B_2)\end{array}}$$

Fig. 1. The allosteric two-state model and the four-ligand allosteric two-state model. The ATSM is presented in the upper left (Hall, 2000). The associated equation presents the response equation Hall developed from this model, color-coded to better illustrate its relationship to the model. The 4L-ATSM, at the lower left, is an extension of the ATSM that can accommodate two orthosteric ligands (A_1 and A_2), and two allosteric ligands (B_1 and B_2) such that there is competition between two ligands at each binding site. The associated equation reflects the response equation for this new model, similarly color-coded to articulate its relationship to the original ATSM response equation. The parameters used in the new model are defined in Table 1.

sponses mediated by the M_3 receptor were used to investigate the PAM activity of amiodarone. Although it initially appeared that amiodarone enhanced ACh action in only one of the responses, we have found that reduction of the magnitude of receptor reserve (by receptor alkylation) reveals similar PAM activity in both measures of response. Finally, by applying simulations generated from the newly developed four-ligand allosteric two-state model (4L-ATSM; Fig. 1), we conclude that amiodarone and its quaternary analog *N*-ethylamiodarone (NEA; Fig. 2) act at a common allosteric site on the extracellular domain of the receptor.

Materials and Methods

Materials. [^{3}H]NMS (82 Ci/mmol) was purchased from PerkinElmer Life and Analytical Sciences (Waltham, MA); [*myo*-^{3}H]inositol (20 Ci/mmol) and [^{3}H]arachidonic acid (AA; 100 Ci/mmol) were purchased from American Radiolabeled Chemicals (St. Louis, MO). *N*-Ethylamiodarone was obtained from IQSynthesis (Maryland Heights, MO). All other reagents were purchased from Sigma-Aldrich (St. Louis, MO).

Cell Culture. CHO cells stably transfected with the human M_3 receptor were used for all binding and response assays. Cells were cultured in F-12 medium supplemented with 5% fetal bovine serum, 100 units/ml penicillin, and 100 μg/ml streptomycin, and growth conditions were 37°C in 5% CO_2 and 100% humidity.

Membrane Preparation. Membranes were collected by harvesting cells in ice-cold 5 mM PB (1 mM KH_2PO_4 and 4 mM Na_2HPO_4, pH 7.4). Cells were homogenized on ice, with three 15-s pulses of a Bio Homogenizer from Biospec Products, Inc. (Bartlesville, OK) and centrifuged at 50,000*g* for 30 min. The supernatant was discarded, and the pellet was resuspended in ice-cold 5 mM PB and stored, in aliquots, at −70°C.

[^{3}H]NMS Binding. For binding experiments, amiodarone was dissolved in dimethyl sulfoxide, the concentration of which was maintained below 1% for all assays; all other reagents were dissolved in buffer or deionized water. Equilibrium binding studies were performed as described previously by Ellis and Seidenberg (1999) and Stahl and Ellis (2010). In brief, these studies were performed in PBS with 1 mM $CaCl_2$ and 1 mM $MgCl_2$, pH 7.4, for 1 h at 25°C. Binding was measured with 1 nM [^{3}H]NMS, and nonspecific binding was determined in the presence of 1 μM atropine. Binding assays were terminated by rapid filtration through GF/B glass fiber filters (pretreated with 0.1% polyethylenimine) on a cell harvester (Brandel Inc., Gaithersburg, MD) to trap membranes, and the filters were rinsed twice with ice-cold 40 mM PB, pH 7.4. Bound radioactivity was measured by liquid scintillation counting (LS6500; Beckman-Coulter, Fullerton, CA).

Intact cell binding was performed by incubating cells with 1 nM [^{3}H]NMS in PBS with 1 mM $CaCl_2$ and 1 mM $MgCl_2$, pH 7.4, for 30 min at 25°C. Nonspecific binding was determined with 3 μM atropine and accounted for approximately 1% of total binding. After the incubation, cells were rinsed twice with PBS and solubilized in 1% SDS; the solubilized cells were transferred to scintillation vials and counted by liquid scintillation counting (LS6500; Beckman-Coulter).

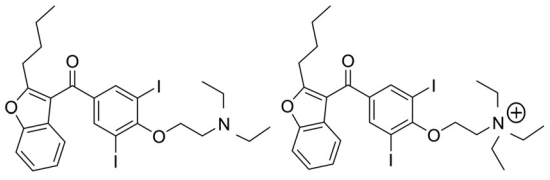

Fig. 2. Molecular structures of the two allosteric ligands used in this study.

[^{3}H]Arachidonic Acid Release. Measurement of [^{3}H]AA release was performed as described in Stahl and Ellis (2010). CHO cells were seeded on 48-well plates (Greiner Bio-One GmbH, Frickenhausen, Germany) at a density of 2.9×10^4 cells/well in 0.25 ml of F-12 medium. Cells were incubated until they attached (approximately 3 h), and the media were exchanged for media containing 0.025 μCi of [^{3}H]AA per well. The cells were then grown for 16 to 20 h before the assay was performed. [^{3}H]AA release was measured in Eagle's basal medium with 20 mM HEPES and 2 mg/ml fatty acid-free bovine serum albumin (EM-BSA). Cells were rinsed twice with EM-BSA, followed by the addition of EM-BSA media containing experimental agents (concentrated stock solutions of all experimental agents were prepared in deionized water) and incubated for 1 h at 37°C. The assay was terminated by aspiration of the media, and the amount of [^{3}H]AA released was determined by liquid scintillation counting (LS6500; Beckman-Coulter).

[^{3}H]Inositol Phosphate Metabolism. The protocol used for measuring inositol phosphate (IP) metabolism was adapted from Ellis et al. (1990) and Bymaster et al. (1999). In brief, cells were cultured in 24-well plates (Falcon; BD Biosciences Discovery Labware, Bedford, MA) at a density of 5×10^4 cells/well in 0.5 ml of F-12 medium. Cells were incubated until they attached, and the media were exchanged for medium containing 2 μCi of [*myo*-^{3}H]inositol per well followed by overnight incubation. The following day, cells were rinsed and incubated in Eagle's basal medium with 20 mM HEPES and 10 mM LiCl for 15 min. After the preincubation, Eagle's basal medium with 20 mM HEPES and 10 mM LiCl and the appropriate experimental agents was added (concentrated stock solutions of all experimental agents were prepared in deionized water), and the assay was allowed to proceed for 30 min at 37°C. After 30 min, the cells were placed on ice, the media were removed, and 0.5 ml of ice-cold methanol was added and allowed to sit for 5 min. Then 0.5 ml of ice-cold water was added to each sample. Before application of the sample, Dowex columns (100–200 mesh) were treated with 3 M ammonium formate in 0.1 M formic acid and rinsed with 0.1 M formic acid. A portion of each sample (0.8 ml) was transferred to a column, after which the columns were rinsed with 0.1 M formic acid and eluted into scintillation vials with 0.8 M ammonium formate in 0.1 M formic acid. The amount of [^{3}H]IP collected was determined by liquid scintillation counting (LS6500; Beckman-Coulter).

Receptor Alkylation. Where noted, receptor number was reduced by treatment with the irreversible antagonist phenoxybenzamine (POB). The protocol was similar to that used by Leff et al. (1993). Specifically, POB was dissolved in ethanol and stored at −20°C. It was diluted in Eagle's basal medium with 20 mM HEPES immediately before use, and the ethanol concentration was maintained below 1%. Cells were incubated in the medium containing POB for 30 min at 37°C. After incubation, two quick washes were performed followed by three 5-min washes. All washes were in Eagle's basal medium with 20 mM HEPES. In the case of measuring IP metabolism, the three 5-min washes were performed in the presence of 10 mM LiCl. After the washes, intact cell binding, AA release, and IP metabolism were measured in the manner described above.

Data Analysis. Binding and response studies were analyzed using the empirical four-parameter equation.

$$Y = \text{Bottom} + \frac{\text{Top} - \text{Bottom}}{1 + 10^{n(\log C_{50} - X)}} \quad (1)$$

where X is the log of the concentration of the ligand used, Y is the amount of binding or response, C_{50} is the concentration of the ligand that produces 50% of the maximal effect, Top and Bottom are the top and bottom plateaus of the curve, and n is related to the Hill slope for the curve. To determine significance in changes of potency and maximal response between curves, the curve fits were evaluated by F test, using Prism (Graphpad Software, Inc., San Diego, CA). The stated parameter values were derived by computer generated curve-

fitting estimates of mean and S.E.M. Where indicated, the *t* test was used to determine significance ($p < 0.05$), based on calculated means and S.E.M. values.

Data from equilibrium binding studies were fit to the allosteric ternary complex model (modified from Ehlert, 1988)

$$Y = \frac{[X][B_{max}]}{[X] + K_X\left(\frac{K_A + [A]}{K_A + \alpha[A]}\right)} \quad (2)$$

where X and A represent the concentrations of the orthosteric and allosteric ligands used, respectively, Y is the amount of binding, K_X and K_A refer to the dissociation constants for each ligand, B_{max} is the value for saturation binding, and α is the binding cooperativity exhibited between the two ligands. In this formulation, $\alpha < 1$ is indicative of negative cooperativity.

The 4L-ATSM presented in Fig. 1 was employed for response simulations. The parameters used to construct the model are defined in Table 1. These parameters represent specific receptor or ligand constants: equilibrium association constants of ligands for their respective sites on the receptor (K and M); intrinsic efficacy values corresponding to a ligand's ability to stabilize the active state of the receptor (α and β); the receptor isomerization constant (L); and two parameters that describe how ligands cooperatively modulate each other's effects on binding or activation (γ and δ). The parameter values used to generate the simulations are stated in Table 2. The equation defines response as the ratio of receptors in the active conformation to the total receptor number, R_{active}/R_{total} (see Appendix). In the simulations based on the model, the parameters of interest are γ and δ. The other parameters are set to values that are reasonable and convenient. For example, K_1 and M_1 are arbitrarily set to 1, L is set to 0.01 to indicate negligible basal activity, and α is set to 100 to indicate robust agonist activity that can be modulated up or down. Finally, β is set to 1 to indicate that the allosteric ligand possesses no agonist activity by itself (in agreement with amiodarone's observed properties).

Results

Amiodarone Allosterically Inhibits [^{3}H]NMS Binding at Muscarinic Receptors. Our previous studies indicated that, at the M_1, M_2, and M_5 subtypes, amiodarone produced incomplete inhibition of [^{3}H]NMS binding. In this study, the inhibition of the binding of 1 nM [^{3}H]NMS was examined at the M_3 subtype. As presented in Fig. 3, amiodarone inhibits [^{3}H]NMS binding with a $\log IC_{50}$ value of -5.3 ± 0.2. In agreement with the previously reported findings, amiodarone inhibits [^{3}H]NMS binding in an incomplete manner, the lower asymptote for inhibition being significantly different from zero. That is, amiodarone inhibits [^{3}H]NMS binding to only approximately 65% of specific binding. Under these conditions, it is possible to determine the affinity of amiodarone ($\log K_A$) and cooperativity between amiodarone and NMS (α) using the TCM (eq. 2). The best-fit values from the model are $\log K_A = -5.8$ and $\alpha = 0.25$.

TABLE 1
Definition of parameters for the four-ligand allosteric two-state model

Parameter Name	Parameter Definition
A_1	[Orthosteric ligand 1]
A_2	[Orthosteric ligand 2]
B_1	[Allosteric ligand 1]
B_2	[Allosteric ligand 2]
K_1	Association constant of A_1
K_2	Association constant of A_2
L	Receptor isomerization constant
M_1	Association constant of B_1
M_2	Association constant of B_2
α_1	Intrinsic efficacy of A_1
α_2	Intrinsic efficacy of A_2
β_1	Intrinsic efficacy of B_1
β_2	Intrinsic efficacy of B_2
γ_{11}	Binding cooperativity between A_1 and B_1
γ_{12}	Binding cooperativity between A_1 and B_2
γ_{21}	Binding cooperativity between A_2 and B_1
γ_{22}	Binding cooperativity between A_2 and B_2
δ_{11}	Activation cooperativity between A_1 and B_1
δ_{12}	Activation cooperativity between A_1 and B_2
δ_{21}	Activation cooperativity between A_2 and B_1
δ_{22}	Activation cooperativity between A_2 and B_2

The Level of Maximal AA Release, for ACh and Pilocarpine, Is Enhanced in the Presence of Amiodarone at M_3 Receptors. In Fig. 4A, 10 μM amiodarone elevates the maximal release of AA elicited via M_3 receptor activation. The maximal response to ACh is elevated by $48 \pm 7.5\%$, and pilocarpine's maximal response is elevated by $105 \pm 5.5\%$ (the maximal response for pilocarpine was $14 \pm 0.8\%$ of the maximum for ACh). In Fig. 4B, 30 μM amiodarone caused elevation of the maximal response of ACh, at M_3, by 70% over acetylcholine alone; this increase was highly significant (see Fig. 4 legend). The ACh potency in the presence of amiodarone ($\log EC_{50} = -6.9 \pm 0.05$) was shifted leftward only slightly with respect to the control curve ($\log EC_{50} = -6.8 \pm 0.07$); this shift did not achieve significance.

TABLE 2
Parameter values used to develop the simulations presented in Fig. 9

Parameter Name	Simulation Values
K_1	1
K_2	1
L	0.01
M_1	1
M_2	1
α_1	100
α_2	1
β_1	1
β_2	1
γ_{11}	0.3
γ_{12}	0.03
γ_{21}	1
γ_{22}	
δ_{11}	10
δ_{12}	1
δ_{21}	1
δ_{22}	

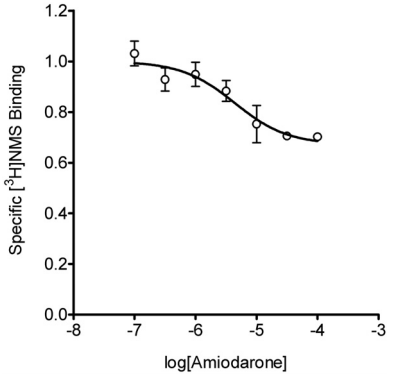

Fig. 3. [^{3}H]NMS equilibrium binding is incompletely inhibited by amiodarone. Amiodarone inhibited [^{3}H]NMS binding at the M_3 receptor. The bottom plateau of the binding inhibition curve is significantly different from zero ($p < 0.0001$). Each point is the average of three experiments expressed as mean ± S.E.M.

Amiodarone Enhances Maximal IP Metabolism Stimulated by Pilocarpine, but Not ACh, at the M_3 Receptor. Amiodarone also exhibited PAM activity on agonist-stimulated IP metabolism. In the case of pilocarpine, amiodarone caused a significant elevation of the maximal level of IP metabolism (Fig. 5A). The logEC_{50} value for pilocarpine was also shifted leftward from -5.9 ± 0.07 to -6.2 ± 0.05 in the presence of amiodarone. Pilocarpine stimulated IP metabolism to $65 \pm 3.3\%$ of the maximal response for ACh. The presence of 30 μM amiodarone did not enhance the maximal response elicited by ACh, but there was a leftward shift in ACh potency of approximately a 2-fold, from logIC_{50} values of -7.4 ± 0.04 to -7.8 ± 0.05 (Fig. 5B). These findings demonstrate that amiodarone affected IP metabolism and AA release in a qualitatively similar manner; in both cases, amiodarone acted as a PAM. However, these studies do raise the question of why the maximal stimulation of IP metabolism by ACh was not enhanced by amiodarone.

IP Response Is Subject to a Larger Receptor Reserve than AA Response. The ability of amiodarone to enhance response in one of the two response assays may be the result of different receptor reserves. This was investigated by determining the maximal response obtained in IP metabolism and AA release, after pretreatment with increasing concentrations of the irreversible antagonist POB. Treatment with POB has been shown to cause a concentration-dependent loss of muscarinic binding sites (Eglen and Harris, 1993; Leff et al., 1993). Confirmation of the presence of a receptor reserve traditionally depends on the demonstration that the ability to produce a response is disproportionately preserved, relative to the loss of receptors. When the receptor reserve is very large, the initial effect of irreversible antagonism is to shift the response curve to the right with negligible loss of maximal response. As greater numbers of receptors are inactivated, the maximal response is attenuated, and the EC_{50} typically approaches the K_A value of the agonist (see Furchgott, 1955). In Fig. 6, maximal response (at saturating agonist concentration) is presented as a function of the fraction of [^{3}H]NMS binding sites remaining after POB pretreatment. We have chosen to analyze this data with an equation that assumes that both binding and response are adequately represented by simple hyperbolic functions. If A is the concentration of agonist and the fractional response, Y, is represented by $A/(A + EC_{50})$, whereas fractional occupancy, X, is represented by $A/(A + K_A)$, then Y can be represented as a function of X,

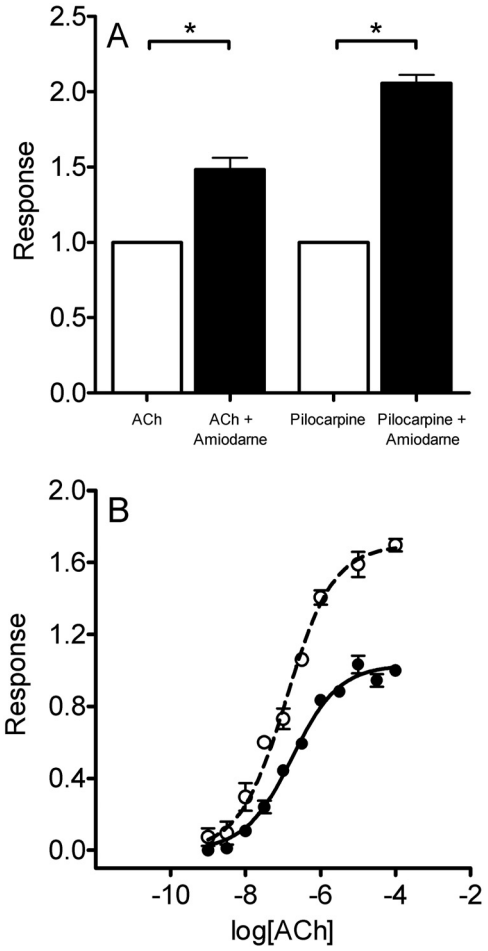

Fig. 4. Amiodarone enhances agonist-stimulated [^{3}H]AA release at the M_3 receptor. A, 10 μM amiodarone displays allosteric effects that cause the elevation of the response stimulated by 100 μM ACh and 1 mM pilocarpine. The effect of amiodarone on the M_3 concentration-response curve of ACh is presented in B. The response stimulated by ACh is presented in the absence (●) and presence (○) of 30 μM amiodarone. Release of [^{3}H]AA stimulated by ACh was elevated in the presence of amiodarone ($p < 0.0001$). ACh potency was slightly enhanced, but this enhancement did not achieve significance. Each point is the average of three experiments expressed as mean ± S.E.M. *, $p < 0.05$.

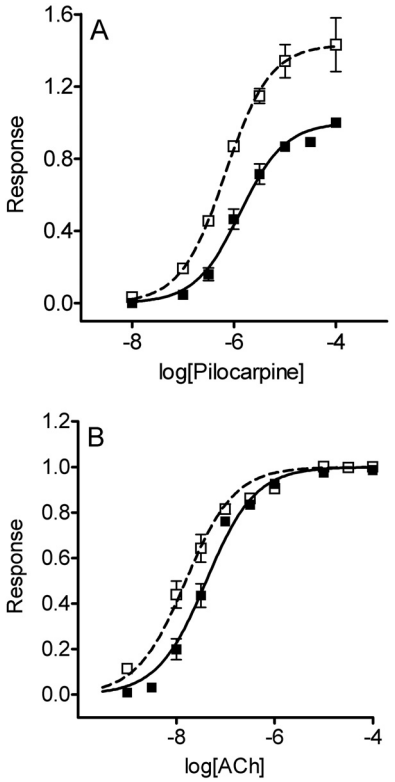

Fig. 5. Amiodarone enhances the maximal stimulation of [^{3}H]IP metabolism induced by pilocarpine at the M_3 receptor. IP metabolism stimulated by pilocarpine (A) and ACh (B) is presented in the absence (■) and presence (□) of 30 μM amiodarone. In the presence of amiodarone, the maximal response stimulated by pilocarpine was elevated, but maximal stimulation by ACh was not enhanced. Amiodarone did cause an increase in potency of both ACh and pilocarpine (see *Results*). Each point is the average of three experiments expressed as mean ± S.E.M.

$$Y = \frac{X}{X(1-r) + r} \quad (3)$$

where $r = EC_{50}/K_A$. When $r = 1$, response is directly proportional to the number of binding sites remaining; the presence of a receptor reserve corresponds to r values that are significantly less than one. One advantage of this approach is that it is not necessary to make assumptions as to whether a given agonist has the same K_A toward different responses (if different responses are due to different conformations of the receptor, there is no reason that K_A must be a shared value; see Hall and Langmead, 2010). Based on eq. 3, the best-fit values were determined for r (Table 3); it is clear that ACh benefits from a much larger receptor reserve in the IP response than it does in the AA response. Of the four curves shown in Fig. 6, only one, the ACh/IP response, can be said to have clearly reached a ceiling of maximal effect. On the other hand, only the pilocarpine/AA response is directly proportional to occupancy (i.e., $r = 1$). Also shown in Table 3 are the EC_{50} values for ACh and pilocarpine at the two responses. In each case, the K_A values are calculated (as EC_{50}/r). Most interestingly, ACh displays a 4-fold higher affinity for the conformation of the receptor that mediates the AA response, relative to the conformation mediating the IP response.

After POB Pretreatment That Significantly Reduces IP and AA Response, Amiodarone Can Potentiate the Maximal Stimulation of Both Responses by ACh. Based on initial studies, 1 μM POB was selected as an effective concentration of pretreatment for investigating the influence of receptor reserve on the response studies. After pretreatment with POB, application of 30 μM amiodarone along with ACh caused a significant elevation of the maximal level of IP metabolism (and AA release, as would be expected) compared with that of ACh alone (Fig. 7A). In light of these findings, a more complete picture of the effects of amiodarone on ACh-stimulated IP metabolism was pursued. Cells were pretreated with POB followed by generation of ACh concentration-response curves in the presence and absence of amiodarone. In Fig. 7B, POB pretreatment caused a right-

TABLE 3
Parameter values obtained from the quantification of receptor reserve in Fig. 6

Response & Agonist	r	$\log EC_{50}$[a]	Calculated $\log K_A$[b]
AA release			
ACh	0.3 ± 0.04*	−6.8 ± 0.07	−6.3
Pilocarpine	1.1 ± 0.14	−5.7 ± 0.04	−5.7
IP metabolism			
ACh	0.02 ± 0.004*	−7.4 ± 0.04	−5.7
Pilocarpine	0.4 ± 0.08*	−5.9 ± 0.07	−5.5

[a] EC_{50} values are from Figs. 4B, 5, A and B, and 8.
[b] K_A values calculated as EC_{50}/r.
* Value significantly different from 1; $P < 0.05$.

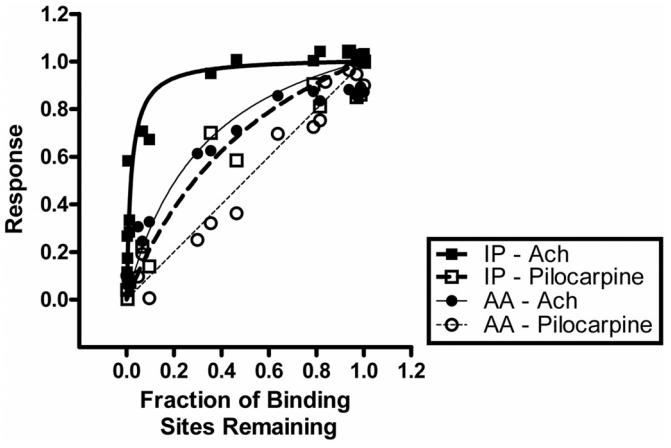

Fig. 6. AA release and IP metabolism exhibit different degrees of receptor reserve. Stimulation of both responses was measured with saturating concentration of a full or partial agonist after pretreatment with POB. These measures of response, after POB treatment, are expressed as a function of the fraction of receptors remaining (measured by binding of 1 nM [^{3}H]NMS to intact cells). For IP metabolism, ACh exhibited a large receptor reserve, whereas the partial agonist pilocarpine experienced a much smaller degree of reserve. For AA release, ACh exhibited a much smaller degree of receptor reserve, similar to that of pilocarpine in IP metabolism. Pilocarpine exhibited no receptor reserve in stimulating AA release. Data points are the individual points from three different experiments. The best-fit curves are generated using eq. 3, and the r values are presented in Table 3.

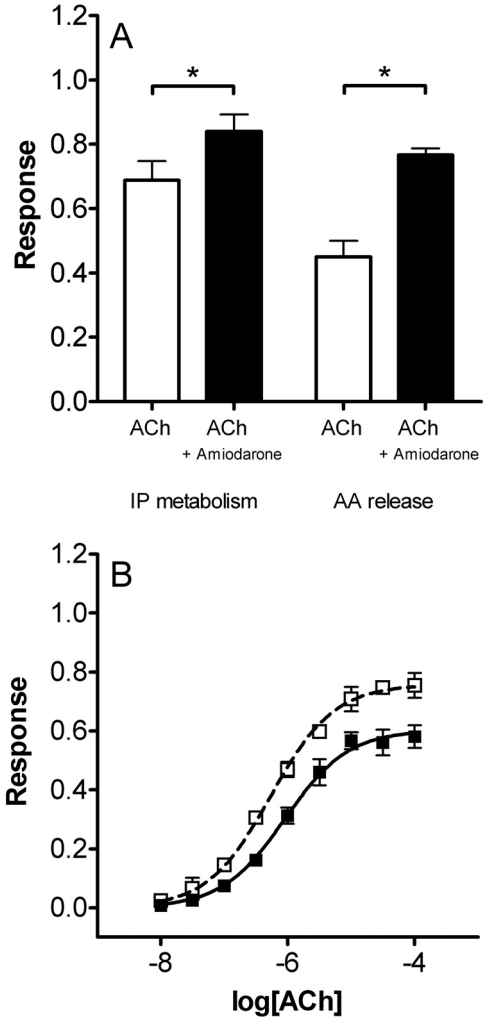

Fig. 7. After POB pretreatment, amiodarone causes elevation of the maximal IP metabolism and AA release stimulated by the M_3 receptor. Pretreatment with 1 μM POB was found to be effective at inhibiting the ACh maximal response. A, upon POB pretreatment, ACh maximal response was inhibited by 32% for IP and 55% for AA release. After pretreatment, amiodarone caused significant elevation of both responses (*, $p < 0.05$). B, ACh concentration-response curves demonstrate the inhibitory effect of POB pretreatment on ACh-mediated IP metabolism (■) and the significant potentiation caused by amiodarone on both ACh potency and maximal response (□; $p < 0.01$). Each point is the average of three experiments expressed as mean ± S.E.M.

ward shift in ACh potency to $\log EC_{50}$ of -6.0 ± 0.06, as would be expected with a marked reduction of the receptor reserve. Amiodarone caused a leftward shift of potency to -6.3 ± 0.05. Amiodarone not only produced enhancement in ACh potency but also elevated the maximal response stimulated by ACh from 60 to 76% of the control maximal response (a relative increase of 25%).

NEA Reverses Amiodarone's Potentiation of Maximal Response at the M_3 Receptor. We wanted to evaluate the interactions between amiodarone and an agonist in the presence of an additional orthosteric or allosteric agent to compare with the predictions of the 4L-ATSM. Stimulation of the AA response by pilocarpine was the preferred choice in these studies because the analysis of receptor reserve had demonstrated that it was in agreement with the occupancy model (Fig. 6). In addition, amiodarone caused a larger enhancement of maximal AA release when pilocarpine was used as the agonist (Fig. 4A). In Fig. 8A, amiodarone enhanced the maximal degree of AA release that pilocarpine was able to induce via the M_3 receptor. The $\log EC_{50}$ of pilocarpine (-5.7 ± 0.04) was not significantly enhanced by the presence of amiodarone. NMS is a competitive antagonist and interacts with the orthosteric binding site on the receptor. As would be expected, NMS caused a rightward shift in the $\log EC_{50}$ of pilocarpine, to -4.2 ± 0.03. NMS also produced a rightward shift in the pilocarpine response curve in the presence of amiodarone ($\log EC_{50}$, -4.3 ± 0.04), but the elevation of the maximal response caused by amiodarone was not affected. The quaternary analog of amiodarone, NEA, was also investigated using this paradigm. NEA (Fig. 8B) caused a parallel rightward shift in the pilocarpine curve of similar magnitude to that caused by NMS ($\log EC_{50}$, -4.0 ± 0.04). However, unlike NMS, NEA markedly attenuated amiodarone's enhancement of the pilocarpine maximal response; NEA shifted the $\log EC_{50}$ for this curve to -4.2 ± 0.03.

Simulations of the 4L-ATSM. The 4L-ATSM (Fig. 1) is a new expansion of the ATSM that describes the functional consequences of two ligands competing at the orthosteric site and two different ligands competing at the allosteric site. In the 4L-ATSM, the central receptor transition ($R \rightleftarrows R^*$) represents the isomerization from the inactive to the active state. The peripheral receptor states indicate multiple bound ligands that can modify that isomerization. The associated equation in Fig. 1 is the functional consequence of the model, color-coded to illustrate the relatedness of the equation to the model and also to Hall's original model (see Appendix for derivation). Simulations were generated from this equation to illustrate the predictions of the model when applied to the experimental paradigms used in Fig. 8. These two paradigms were 1) the presence of one allosteric and two orthosteric ligands and 2) the presence of one orthosteric and two allosteric ligands. The parameter values in Table 2 were selected so that the theoretical ligands would be comparable with pilocarpine (A_1), NMS (A_2), amiodarone (B_1), and NEA (B_2).

Competition between an orthosteric agonist and a neutral orthosteric antagonist causes a rightward shift in the agonist concentration-response curve; this characteristic is evident in the simulation shown in Fig. 9A. The orthosteric antagonist also produces the expected rightward shift in the presence of a PAM that elevates maximal response, but the orthosteric antagonist does not reverse the elevation of the upper asymptote caused by the PAM. Conversely, competition between two ligands at a common allosteric site will produce response curves of a much different nature (Fig. 9B).

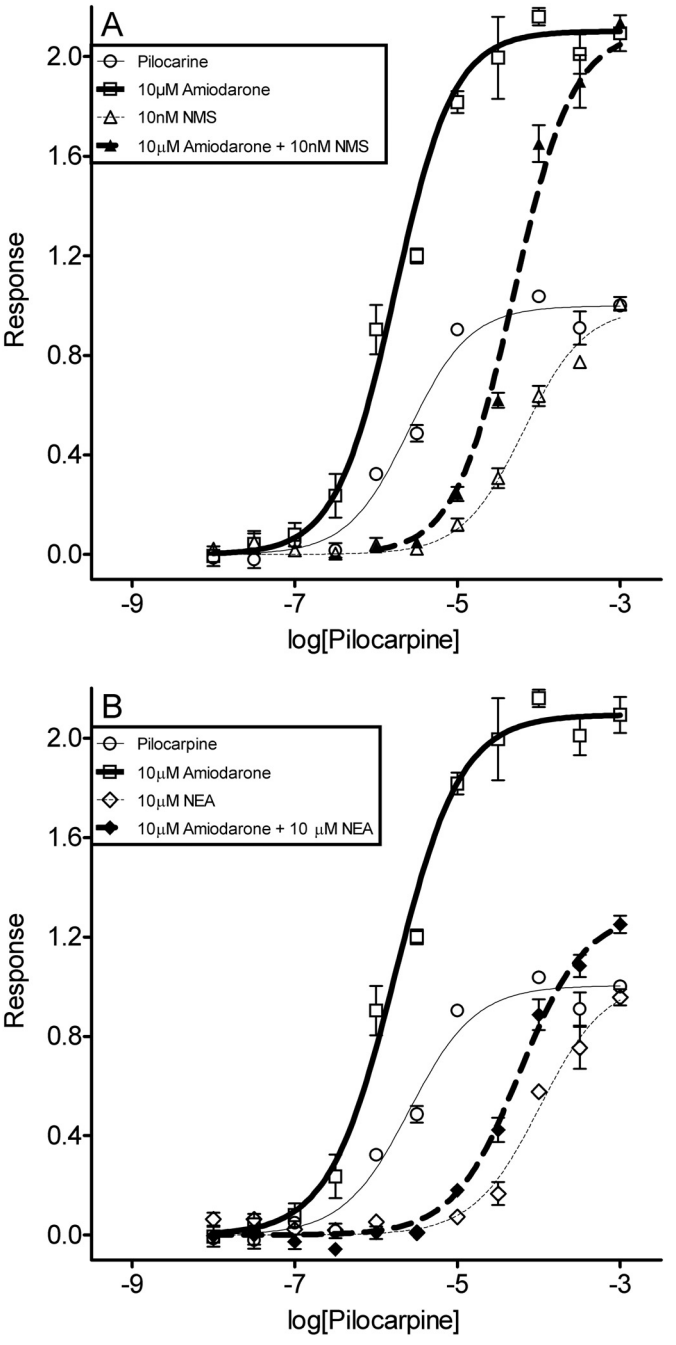

Fig. 8. NEA and NMS exhibit qualitative differences in their modulation of amiodarone's effect. In A and B, the [^{3}H]AA release mediated by pilocarpine at M_3 is presented in the absence (○) and presence (□) of 10 μM amiodarone. Amiodarone caused an increase in the maximal response without a significant change in pilocarpine potency. A, the concentration-response curve of pilocarpine was rightward-shifted by the competitive antagonist NMS (△). In the presence of amiodarone, NMS caused a similar rightward shift in the response curve but did not reduce the enhancement of maximal response caused by amiodarone (▲). B, 10 μM NEA caused a rightward shift in the concentration-response curve of pilocarpine (◇). The pilocarpine response curve in the presence of amiodarone was also shifted rightward by NEA and, moreover, the enhancement of maximal response caused by amiodarone was markedly attenuated by NEA (◆). Each point is the average of three experiments expressed as mean ± S.E.M.

The presence of the negative allosteric modulator (NAM) causes a rightward shift from the control agonist response curve. When the same inhibitory concentration is applied to agonist response, in the presence of the PAM, it is clear that this interaction differs from the case of the orthosteric antagonist. In this PAM + NAM curve, the elevation of the upper asymptote is attenuated by the presence of the NAM because of the competition for occupancy of the common allosteric site. The striking similarities between these simulations and the experimental data in Fig. 8 reinforce the expectation (based on their common structure) that amiodarone and NEA compete at a common allosteric site.

Discussion

The ability of amiodarone to inhibit the binding of [^{3}H]NMS to M_1, M_2, and M_5 muscarinic receptors has been reported previously (Stahl and Ellis, 2010). The present work extends the study of amiodarone's effects on binding to include the M_3 subtype (Fig. 3). In agreement with the proposed allosteric mechanism of action, amiodarone does not completely inhibit binding at the M_3 subtype. Incomplete binding inhibition is convincing evidence that a ligand does not compete for the same site as the radioligand (Christopoulos and Kenakin, 2002). In the application of allosteric theory, the focus has usually been on binding cooperativity, a point embodied in the TCM in which the binding cooperativity is a shared modulatory value that the two ligands possess when they are bound to a common receptor. However, it is recognized that allosteric ligands are capable of modulating efficacy (Ehlert, 1988), and a number of groups have observed allosteric modulation of agonist efficacy at GPCRs (Urwyler et al., 2003; Sharma et al., 2008; Bridges et al., 2009). Our previous studies found that amiodarone was able to allosterically enhance agonist-stimulated response at the M_5 receptor, without any potency enhancement. We have now demonstrated that amiodarone potentiates AA release mediated by the M_3 receptor (Fig. 4). This enhancement in maximal response was accompanied by a trend toward a leftward shift in ACh potency. These findings demonstrate that amiodarone affects M_3- and M_5-mediated responses similarly.

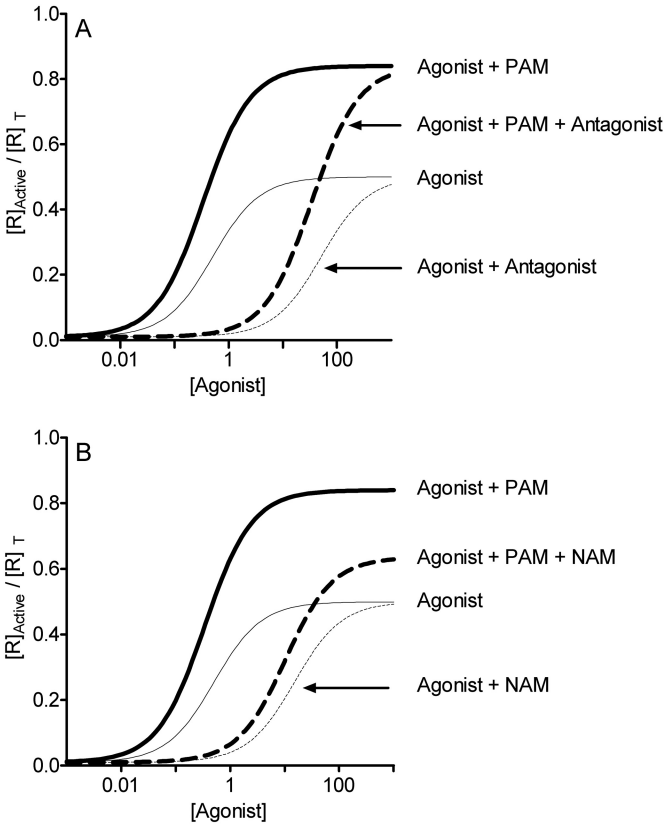

Fig. 9. Simulations of the 4L-ATSM illustrate the effects of competition at either the orthosteric or allosteric site. In A and B, the effects of an agonist alone are represented by the solid thin line, whereas the effects of the agonist in the presence of a PAM that elevates maximal response are represented by the thick solid line. A, a competitive antagonist causes a rightward shift in the agonist response curve in the presence (thick dashed line) and absence (thin dotted line) of the PAM. The competitive antagonist is not able to reverse the enhancement of the upper asymptote caused by the PAM. B, a NAM that is neutral on efficacy causes a rightward shift in the agonist response curve in the absence (thin dotted line) and presence (thick dashed line) of a PAM. It is noteworthy that the enhancement of the upper asymptote caused by the PAM is reversed by the NAM. Table 2 indicates the parameter values that were applied to the 4L-ATSM equation in Fig. 1 for these simulations.

In this study, we show that amiodarone causes elevation of maximal ACh-mediated AA release but not maximal ACh-mediated IP metabolism (Figs. 4B and 5A). One explanation for differential potentiation is that IP metabolism is subject to a large receptor reserve, and the maximal response is therefore not able to be elevated, whereas stimulation of AA release is not subject to such a significant receptor reserve. The ability of amiodarone to enhance both responses elicited by the partial agonist pilocarpine is in agreement with this concept. The finding of markedly different reserves suggests in turn that the two responses are independent, not sequential. Furthermore, ACh displays different K_A values for the responses (Table 3); this implies that different conformations of the receptor are responsible for the two responses. In fact, a large body of evidence in the literature demonstrates the independence of these responses. For example, Burch et al. (1986) found that both responses were linked to α_1-adrenergic receptors via G proteins, but that different agents could inhibit one response without affecting the other. Conklin et al. (1988) reported that short-term treatment of A9L cells with the protein kinase C activator phorbol 12-myristate 13-acetate inhibited the activation of IP metabolism by M_3 receptors but enhanced the muscarinic AA response. Perez et al. (1996) identified a mutation in α_{1B}-adrenergic receptors that induced constitutive activity in the IP response, although the AA response was unaffected. Kurrasch-Orbaugh et al. (2003a) found that different $5HT_{2A}$ receptor agonists possessed opposite functional selectivity for the two responses in NIH-3T3 cells; indeed, these authors also found different magnitudes of receptor reserve for the two responses. Finally, Berg et al. (1998) found that $5HT_{2C}$ agonists possessed different affinities for the active states that lead to IP and AA responses in CHO cells. These authors suggested that these different affinities are the cause of the phenomenon known as agonist-directed trafficking of receptor stimulus.

It is worth noting that the use of screening assays that exhibit large receptor reserves may preclude the discovery of PAMs with properties similar to those of amiodarone. That is, the ability of amiodarone to enhance the maximal IP response elicited by ACh was not apparent until the reserve was eliminated. This may be one reason why allosteric mod-

ulators that elevate maximal response without altering potency to a significant extent are so rarely discovered. In addition, the sensitivity of this type of PAM to the degree of receptor reserve may present therapeutic advantages in some cases. For example, if a pathological condition was caused by a loss of receptors in a particular tissue that resulted in a significant reduction in the receptor reserve, such a PAM could enhance response in the affected tissue, although tissues with intact receptor reserves would be unaffected.

The remaining question is why amiodarone is so effective at enhancing the maximal effect of ACh in the AA response, even though there is an indication of some receptor reserve. The likely answer is simply that the degree of reserve is small. Comparison of the ACh/IP curve to the ACh/AA curve in Fig. 6 illustrates that the IP response clearly reaches a ceiling as more and more receptors are left intact; the AA response possess no such ceiling effect. However, there is a further possibility. Studies have indicated that GPCRs are capable of differentially activating multiple G proteins (e.g., Akam et al., 2001) and that receptor-mediated AA release is mediated by multiple parallel pathways that are initiated by distinct G proteins (Kurrasch-Orbaugh et al., 2003b; Hecquet et al., 2006). It is possible that a larger receptor reserve is associated with one of these pathways and that amiodarone acts predominantly on the pathway with the smaller degree of reserve. Further studies will be required to address this possibility.

As described under *Introduction*, the ATSM is a mechanistic model that is useful for understanding response modulation in the presence of an allosteric ligand. Two of the parameters of the model, binding cooperativity (γ) and activation cooperativity (δ), represent the forms of modulation an allosteric ligand may induce on agonist response curves. That is, positive values of either parameter will cause an enhancement of agonist potency, and positive activation cooperativity may additionally cause an enhancement of maximal response if there is not a system-dependent limit to response. Studies of the effects of amiodarone on agonist-stimulated [^{3}H]AA release at the M_3 receptor (Fig. 8) were compared with simulations based on the response equation of the 4L-ATSM (Fig. 9). The simulations demonstrate that the 4L-ATSM is capable of elegantly replicating the ability of amiodarone to enhance maximal response without enhancing agonist potency; this is accomplished by stipulating a *positively* cooperative δ and *negatively* cooperative γ, each of which counterbalances the other's effect on potency (see Table 2). Of course, in the case of a single orthosteric and allosteric ligand, the 4L-ATSM reduces to the ATSM. Hall (2000) used the ATSM to simulate the opposite case, where efficacy is reduced because of a negative δ, but potency is unchanged because of a positive γ, to replicate results obtained by Litschig et al. (1999) at the metabotropic glutamate receptor metabotropic glutamate receptor 1. In a similar set of findings, Price et al. (2005) demonstrated an allosteric inhibition of maximal response combined with an increase in agonist potency.

The most striking effect of amiodarone is its ability to enhance the maximal responses elicited by acetylcholine and pilocarpine. The quaternary analog NEA lacks this property entirely. Sharma et al. (2008) reported a similar switch from positive to negative allosteric modulation caused by differential methylation of adjacent positions in a phenyl ring in a series of metabotropic glutamate receptor 5 ligands. They termed this a "molecular switch" in the compound and noted that allosteric modulators can be especially sensitive to dramatic shifts in pharmacological properties as a result of slight changes in structure. Indeed, NEA simply shifts the agonist concentration-response curves to lower apparent potency in a manner that superficially resembles the effect produced by the orthosteric antagonist NMS (Fig. 8). Based on their close chemical structures, NEA would be expected to act at the same site at which amiodarone acts. The ATSM is well suited to describing response cooperativity between one allosteric ligand and one orthosteric ligand, as we have emphasized above. In order to quantitatively describe and compare the behavior expected of an antagonist such as NMS, which interacts competitively at the orthosteric site, with an allosteric antagonist that interacts competitively with amiodarone at its allosteric site, a more expansive model was needed. Fortunately, as noted under *Introduction*, the ATSM shares with the CTCM the feature that it can readily be generalized. We have expanded the cubic ATSM to a tetracubic model that accommodates two orthosteric ligands and two allosteric ligands simultaneously; we call this four-ligand version of the model the 4L-ATSM. The two models and their equations of response are presented in a color-coded manner in Fig. 1 to permit visual appreciation of the relationships between the models and also to articulate the relationship between the models and their respective equations. Simulations based on the 4L-ATSM used parameter values consistent with an orthosteric agonist (A_1), an orthosteric antagonist (A_2), an allosteric ligand that promotes positive activation cooperativity but negative binding cooperativity with A_1 (B_1), and an allosteric ligand that promotes only negative binding cooperativity with A_1 (B_2). The curves resulting from these simulations are consistent with the experimental data and reinforce the expectation that amiodarone and NEA interact with a common allosteric site. Furthermore, the quaternary nature of NEA indicates that this site lies on the extracellular portion of the receptor.

In conclusion, amiodarone interacts with a novel allosteric site on muscarinic receptors. In the present study, we have focused on characterizing the ability of amiodarone to act as a PAM on responses elicited by activation of the M_3 receptor. This PAM activity is expressed as an elevation of maximal response, with little or no enhancement of agonist potency. In terms of Hall's ATSM, this is accomplished by simultaneous positive activation cooperativity and negative binding cooperativity. Most interestingly, amiodarone's PAM activity is readily apparent in the AA response, but not in the IP response. However, when the receptor reserve for the latter response is dramatically reduced, amiodarone's ability to enhance the maximal response of ACh is unmasked. Furthermore, the determination of the magnitude of the receptor reserve allowed for the calculation of agonist affinity (K_A) and demonstrated that ACh has greater affinity for the conformation of the receptor that is associated with the AA response. Finally, the amiodarone analog NEA lacks amiodarone's positive activation cooperativity but exhibits negative binding cooperativity. The ability of NEA to reverse the PAM effects of amiodarone is consistent with these two ligands competing at a common allosteric site.

Appendix

Response. Following the law of conservation of mass, the following equation defines the total population of receptors, $[R]_{total}$ as all of the possible permutations of receptor states that the presence of four ligands can produce.

$$\begin{aligned}[R]_{total} = {} & [R]+[A_1R]+[A_2R]+[RB_1]+[RB_2] \\ & +[A_1RB_1]+[A_1RB_2]+[A_2RB_1]+[A_2RB_2] \\ & +[R^*]+[A_1R^*]+[A_2R^*]+[R^*B_1]+[R^*B_2] \\ & +[A_1R^*B_1]+[A_1R^*B_2]+[A_2R^*B_1]+[A_2R^*B_2]\end{aligned}$$

The parameters in Table 1 can be used to substitute terms in the previous equation as

$$\begin{aligned}[R]_{total} = {} & [R](1+K_1[A_1]+K_2[A_2]+M_1[B_1]+M_2[B_2] \\ & +\gamma_{11}K_1M_1[A_1][B_1]+\gamma_{12}K_1M_2[A_1][B_2] \\ & +\gamma_{21}K_2M_1[A_2][B_1]+\gamma_{22}K_2M_2[A_2][B_2] \\ & +L(1+\alpha_1K_1[A_1]+\alpha_2K_2[A_2]+\beta_1M_1[B_1]+\beta_2M_2[B_2] \\ & +\alpha_1\beta_1\gamma_{11}\delta_{11}K_1M_1[A_1][B_1]+\alpha_1\beta_2\gamma_{12}\delta_{12}K_1M_2[A_1][B_2] \\ & +\alpha_2\beta_1\gamma_{21}\delta_{21}K_2M_1[A_2][B_1]+\alpha_2\beta_2\gamma_{22}\delta_{22}K_2M_2[A_2][B_2]))\end{aligned}$$

In the model, response is defined as the sum of all of the active conformations of the receptor, $[R]_{active}$ (R^*, A_1R^*, B_1R^*, etc.). A mathematical expression of response can then be defined as the fraction of the total receptor population, $[R]_T$, that exists in the active conformation:

$$\frac{[R]_{active}}{[R]_{total}}=\frac{\begin{array}{c}[R^*]+[A_1R^*]+[A_2R^*]+[R^*B_1]+[R^*B_2] \\ +[A_1R^*B_1]+[A_1R^*B_2]+[A_2R^*B_1]+[A_2R^*B_2]\end{array}}{\begin{array}{c}[R]+[A_1R]+[A_2R]+[RB_1]+[RB_2] \\ +[A_1RB_1]+[A_1RB_2]+[A_2RB_1]+[A_2RB_2] \\ +[R^*]+[A_1R^*]+[A_2R^*]+[R^*B_1]+[R^*B_2] \\ +[A_1R^*B_1]+[A_1R^*B_2]+[A_2R^*B_1]+[A_2R^*B_2]\end{array}}$$

This equation is also amenable to substitution in a manner similar to that above:

$$\frac{[R]_{active}}{[R]_{total}}=$$

$$\frac{\begin{array}{c}L+\alpha_1K_1L[A_1]+\alpha_2K_2L[A_2]+\beta_1M_1L[B_1]+\beta_2M_2L[B_2] \\ +\alpha_1\beta_1\gamma_{11}\delta_{11}K_1LM_1[A_1][B_1]+\alpha_1\beta_2\gamma_{12}\delta_{12}K_1LM_2[A_1][B_2] \\ +\alpha_2\beta_1\gamma_{21}\delta_{21}K_2LM_1[A_2][B_1]+\alpha_2\beta_2\gamma_{22}\delta_{22}K_2LM_2[A_2][B_2]\end{array}}{\begin{array}{c}1+K_1[A_1]+K_2[A_2]+M_1[B_1]+M_2[B_2] \\ +\gamma_{11}K_1M_1[A_1][B_1]+\gamma_{12}K_1M_2[A_1][B_2] \\ +\gamma_{21}K_2M_1[A_2][\mathrm{B}_1]+\gamma_{22}K_2M_2[A_2][B_2] \\ +\mathrm{L}+\alpha_1K_1L[A_1]+\alpha_2K_2L[A_2]+\beta_1M_1L[B_1]+\beta_2M_2L[B_2] \\ +\alpha_1\beta_1\gamma_{11}\delta_{11}K_1M_1L[A_1][B_1]+\alpha_1\beta_2\gamma_{12}\delta_{12}K_1M_2L[A_1][B_2] \\ +\alpha_2\beta_1\gamma_{21}\delta_{21}K_2M_1L[A_2][B_1]+\alpha_2\beta_2\gamma_{22}\delta_{22}K_2M_2L[A_2][B_2]\end{array}}$$

This equation can be further simplified:

$$\frac{[R]_{active}}{[R]_{total}}=\frac{\begin{array}{c}L(1+\beta_1M_1[B_1]+\beta_2M_2[B_2] \\ +\alpha_1K_1[A_1](1+\beta_1\gamma_{11}\delta_{11}M_1[B_1]+\beta_2\gamma_{12}\delta_{12}M_2[B_2]) \\ +\alpha_2K_2[A_2](1+\beta_1\gamma_{21}\delta_{21}M_1[B_1]+\beta_2\gamma_{22}\delta_{22}M_2[B_2]))\end{array}}{\begin{array}{c}1+M_1[B_1]+M_2[B_2] \\ +K_1[A_1](1+\gamma_{11}M_1[B_1]+\gamma_{12}M_2[B_2]) \\ +K_2[A_2](1+\gamma_{21}M_1[B_1]+\gamma_{22}M_2[B_2]) \\ +L(1+\beta_1M_1[B_1]+\beta_2M_2[B_2] \\ +\alpha_1K_1[A_1](1+\beta_1\gamma_{11}\delta_{11}M_1[B_1]+\beta_2\gamma_{12}\delta_{12}M_2[B_2]) \\ +\alpha_2K_2[A_2](1+\beta_1\gamma_{21}\delta_{21}M_1[B_1]+\beta_2\gamma_{22}\delta_{22}M_2[B_2]))\end{array}}$$

Binding. The equation that expresses ligand binding is comparable with that used for receptor response in that it identifies a subset of receptor states as those relevant for investigation. The important receptor states in binding experiments are all those labeled with the orthosteric radioligand A_1 (i.e., A_1R, A_1RB_1, etc.). All of the possible states of bound orthosteric radioligand are expressed as follows:

$$[A_1]_{bound}=[A_1R],[A_1RB_1],[A_1RB_2],[A_1R^*],[A_1R^*B_1],[A_1R^*B2_2]$$

From this definition of bound receptor forms, the fractional occupancy of the radioligand can be expressed:

$$\frac{[A_1]_{bound}}{[R]_{total}}=$$

$$\frac{[A_1R],[A_1RB_1],[A_1RB_2],[A_1R^*],[A_1R^*B_1],[A_1R^*B_2]}{\begin{array}{c}[R]+[A_1R]+[A_2R]+[RB_1]+[RB_2]+[A_1RB_1]+[A_1RB_2] \\ +[A_2RB_1]+[A_2RB_2]+[R^*]+[A_1R^*]+[A_2R^*]+[R^*B_1] \\ +[R^*B_2]+[A_1R^*B_1]+[A_1R^*B_2]+[A_2R^*B_1]+[A_2R^*B_2]\end{array}}$$

Using the parameters expressed in Table 1, the previous equation can be rewritten:

$$\frac{[A_1]_{bound}}{[R]_{total}}=$$

$$\frac{\begin{array}{c}K_1[A_1]+\gamma_{11}K_1[A_1]M_1[B_1]+\gamma_{12}K_1[A_1]M_2[B_2]+\alpha_1K_1[A_1]L \\ +\alpha_1\beta_1\gamma_{11}\delta_{11}K_1[A_1]M_1[B_1]L+\alpha_1\beta_2\gamma_{12}\delta_{12}K_1[A_1]M_2[B_2]L\end{array}}{\begin{array}{c}1+K_1[A_1]+K_2[A_2]+M_1[B_1]+M_2[B_2] \\ +\gamma_{11}K_1[A_1]M_1[B_1]+\gamma_{12}K_1[A_1]M_2[B_2] \\ +\gamma_{21}K_2[A_2]M_1[B_1]+\gamma_{22}K_2[A_2]M_2[B_2] \\ +L+\alpha_1K_1[A_1]L+\alpha_2K_2[A_2]L+\beta_1M_1[B_1]L+\beta_2M_2[B_2]L \\ +\alpha_1\beta_1\gamma_{11}\delta_{11}K_1[A_1]M_1[B_1]L+\alpha_1\beta_2\gamma_{12}\delta_{12}K_1[A_1]M_2[B_2]L \\ +\alpha_2\beta_1\gamma_{21}\delta_{21}K_2[A_2]M_1[B_1]L+\alpha_2\beta_2\gamma_{22}\delta_{22}K_2[A_2]M_2[B_2]L\end{array}}$$

This equation can be simplified:

$$\frac{[A_1]_{bound}}{[R]_{total}}=\frac{\begin{array}{c}K_1[A_1](1+\gamma_{11}M_1[B_1]+\gamma_{12}M_2[B_2] \\ +\alpha_1L(1+\beta_1\gamma_{11}\delta_{11}M_1[B_1]+\beta_2\gamma_{12}\delta_{12}M_2[B_2]))\end{array}}{\begin{array}{c}1+K_1[A_1]+K_2[A_2]+M_1[B_1]+M_2[B_2] \\ +K_1[A_1](\gamma_{11}M_1[B_1]+\gamma_{12}M_2[B2]) \\ +K_2[A_2](\gamma_{21}M_1[B_1]+\gamma_{22}M_2[B_2]) \\ +L(1+\alpha_1K_1[A_1]+\alpha_2K_2[A_2]+\beta_1M_1[B_1]+\beta_2M_2[B_2] \\ +\alpha_1K_1[A_1](\beta_1\gamma_{11}\delta_{11}M_1[B_1]+\beta_2\gamma_{12}\delta_{12}M_2[B_2]) \\ +\alpha_2K_2[A](\beta_1\gamma_{21}\delta_{21}M_1[B_1]+\beta_2\gamma_{22}\delta_{22}M_2[B_2))\end{array}}$$

Authorship Contributions

Participated in research design: Stahl, Elmslie, and Ellis.
Conducted experiments: Stahl and Elmslie.
Contributed new reagents or analytic tools: Stahl and Ellis.
Performed data analysis: Stahl, Elmslie, and Ellis.
Wrote or contributed to the writing of the manuscript: Stahl, Elmslie, and Ellis.

References

Akam EC, Challiss RA, and Nahorski SR (2001) G(q/11) and G(i/o) activation profiles in CHO cells expressing human muscarinic acetylcholine receptors: dependence on agonist as well as receptor-subtype. *Br J Pharmacol* **132:**950–958.
Berg K_A, Maayani S, Goldfarb J, Scaramellini C, Leff P, and Clarke WP (1998) Effector pathway-dependent relative efficacy at serotonin type 2A and 2C receptors: evidence for agonist-directed trafficking of receptor stimulus. *Mol Pharmacol* **54:**94–104.
Bridges TM and Lindsley CW (2008) G-protein-coupled receptors: from classical modes of modulation to allosteric mechanisms. *ACS Chem Biol* **3:**530–541.
Bridges TM, Marlo JE, Niswender CM, Jones CK, Jadhav SB, Gentry PR, Plumley HC, Weaver CD, Conn PJ, and Lindsley CW (2009) Discovery of the first highly M5-preferring muscarinic acetylcholine receptor ligand, an M5 positive allosteric modulator derived from a series of 5-trifluoromethoxy N-benzyl isatins. *J Med Chem* **52:**3445–3448.
Burch RM, Luini A, and Axelrod J (1986) Phospholipase A2 and phospholipase C are activated by distinct GTP-binding proteins in response to alpha 1-adrenergic stimulation in FRTL5 thyroid cells. *Proc Natl Acad Sci USA* **83:**7201–7205.

Bymaster FP, Calligaro DO, and Falcone JF (1999) Arachidonic acid release in cell lines transfected with muscarinic receptors: a simple functional assay to determine response of agonists. *Cell Signal* **11:**405–413.
Christopoulos A and Kenakin T (2002) G protein-coupled receptor allosterism and complexing. *Pharmacol Rev* **54:**323–374.
Conklin BR, Brann MR, Buckley NJ, Ma AL, Bonner TI, and Axelrod J (1988) Stimulation of arachidonic acid release and inhibition of mitogenesis by cloned genes for muscarinic receptor subtypes stably expressed in A9 L cells. *Proc Natl Acad Sci USA* **85:**8698–8702.
Eglen RM and Harris GC (1993) Selective inactivation of muscarinic M2 and M3 receptors in guinea-pig ileum and atria in vitro. *Br J Pharmacol* **109:**946–952.
Ehlert FJ (1988) Estimation of the affinities of allosteric ligands using radioligand binding and pharmacological null methods. *Mol Pharmacol* **33:**187–194.
Ehlert FJ (2005) Analysis of allosterism in functional assays. *J Pharmacol Exp Ther* **315:**740–754.
Ellis J (1997) Allosteric binding sites on muscarinic receptors. *Drug Dev Res* **40:**193–204.
Ellis J, Huyler JH, Kemp DE, and Weiss S (1990) Muscarinic receptors and second-messenger responses of neurons in primary culture. *Brain Res* **511:**234–240.
Ellis J and Seidenberg M (1999) Competitive and allosteric interactions of 6-chloro-5,10-dihydro-5-[(1-methyl-4-piperidinyl)acetyl]-11*H*-di benzo[*b*,*e*][1,4]diazepine-11-one hydrochloride (UH-AH 37) at muscarinic receptors, via distinct epitopes. *Biochem Pharmacol* **57:**181–186.
Ellis J and Seidenberg M (2000) Interactions of alcuronium, TMB-8, and other allosteric ligands with muscarinic acetylcholine receptors: studies with chimeric receptors. *Mol Pharmacol* **58:**1451–1460.
Furchgott RF (1955) The pharmacology of vascular smooth muscle. *Pharmacol Rev* **7:**183–265.
Hall DA (2000) Modeling the functional effects of allosteric modulators at pharmacological receptors: an extension of the two-state model of receptor activation. *Mol Pharmacol* **58:**1412–1423.
Hall DA and Langmead CJ (2010) Matching models to data: a receptor pharmacologist's guide. *Br J Pharmacol* **161:**1276–1290.
Hecquet C, Biyashev D, Tan F, and Erdös EG (2006) Positive cooperativity between the thrombin and bradykinin B2 receptors enhances arachidonic acid release. *Am J Physiol Heart Circ Physiol* **290:**H948–H958.
Jones SVP, Levey AI, Weiner DM, Ellis J, Novotny E, Yu S-H, Dorje F, Wess J and Brann MR (1992) Muscarinic acetylcholine receptors, in *Molecular Biology of Receptors Which Couple to G-Proteins* (Brann MR ed), Birkauser Boston Inc., Cambridge, MA.
Kurrasch-Orbaugh DM, Parrish JC, Watts VJ, and Nichols DE (2003a) A complex signaling cascade links the serotonin2A receptor to phospholipase A2 activation: the involvement of MAP kinases. *J Neurochem* **86:**980–991.
Kurrasch-Orbaugh DM, Watts VJ, Barker EL, and Nichols DE (2003b) Serotonin 5-hydroxytryptamine 2A receptor-coupled phospholipase C and phospholipase A2 signaling pathways have different receptor reserves. *J Pharmacol Exp Ther* **304:**229–237.
Langmead CJ, Watson J, and Reavill C (2008) Muscarinic acetylcholine receptors as CNS drug targets. *Pharmacol Ther* **117:**232–243.
Leff P (1995) The two-state model of receptor activation. *Trends Pharmacol Sci* **16:**89–97.
Leff P, Dougall IG, and Harper D (1993) Estimation of partial agonist affinity by interaction with a full agonist: a direct operational model-fitting approach. *Br J Pharmacol* **110:**239–244.
Litschig S, Gasparini F, Rueegg D, Stoehr N, Flor PJ, Vranesic I, Prézeau L, Pin JP, Thomsen C, and Kuhn R (1999) CPCCOEt, a noncompetitive metabotropic glutamate receptor 1 antagonist, inhibits receptor signaling without affecting glutamate binding. *Mol Pharmacol* **55:**453–461.
Marlo JE, Niswender CM, Days EL, Bridges TM, Xiang Y, Rodriguez AL, Shirey JK, Brady AE, Nalywajko T, Luo Q, et al. (2009) Discovery and characterization of novel allosteric potentiators of M1 muscarinic receptors reveals multiple modes of activity. *Mol Pharmacol* **75:**577–588.
May LT, Leach K, Sexton PM, and Christopoulos A (2007) Allosteric modulation of G protein-coupled receptors. *Annu Rev Pharmacol Toxicol* **47:**1–51.
Perez DM, Hwa J, Gaivin R, Mathur M, Brown F, and Graham RM (1996) Constitutive activation of a single effector pathway: evidence for multiple activation states of a G protein-coupled receptor. *Mol Pharmacol* **49:**112–122.
Price MR, Baillie GL, Thomas A, Stevenson LA, Easson M, Goodwin R, McLean A, McIntosh L, Goodwin G, Walker G, et al. (2005) Allosteric modulation of the cannabinoid CB1 receptor. *Mol Pharmacol* **68:**1484–1495.
Sharma S, Rodriguez AL, Conn PJ, and Lindsley CW (2008) Synthesis and SAR of a mGluR5 allosteric partial antagonist lead: unexpected modulation of pharmacology with slight structural modifications to a 5-(phenylethynyl)pyrimidine scaffold. *Bioorg Med Chem Lett* **18:**4098–4101.
Shirey JK, Xiang Z, Orton D, Brady AE, Johnson K_A, Williams R, Ayala JE, Rodriguez AL, Wess J, Weaver D, et al. (2008) An allosteric potentiator of M4 mAChR modulates hippocampal synaptic transmission. *Nat Chem Biol* **4:**42–50.
Stahl E and Ellis J (2010) Novel allosteric effects of amiodarone at the muscarinic M5 receptor. *J Pharmacol Exp Ther* **334:**214–222.
Stockton JM, Birdsall NJ, Burgen AS, and Hulme EC (1983) Modification of the binding properties of muscarinic receptors by gallamine. *Mol Pharmacol* **23:**551–557.
Tränkle C, Weyand O, Voigtländer U, Mynett A, Lazareno S, Birdsall NJ, and Mohr K (2003) Interactions of orthosteric and allosteric ligands with [3H]dimethyl-W84 at the common allosteric site of muscarinic M2 receptors. *Mol Pharmacol* **64:**180–190.
Urwyler S, Pozza MF, Lingenhoehl K, Mosbacher J, Lampert C, Froestl W, Koller M, and Kaupmann K (2003) *N*,*N*′-Dicyclopentyl-2-methylsulfanyl-5-nitro-pyrimidine-4,6-diamine (GS39783) and structurally related compounds: novel allosteric enhancers of gamma-aminobutyric acidB receptor function. *J Pharmacol Exp Ther* **307:**322–330.
Weiss JM, Morgan PH, Lutz MW, and Kenakin TP (1996) The cubic ternary complex receptor-occupancy model. I. Model description. *J Theor Biol* **178:**151–167.
Wess J, Eglen RM, and Gautam D (2007) Muscarinic acetylcholine receptors: mutant mice provide new insights for drug development. *Nat Rev Drug Discov* **6:**721–733.

Address correspondence to: John Ellis, Department of Psychiatry, H073, Hershey Medical Center, Penn State University College of Medicine, 500 University Dr., Hershey, PA 17033. E-mail: johnellis@psu.edu